

Validating the performance of direct fastening (PAF) into concrete with high-speed measuring technology

Ronja Scholz¹ | Pascal Franck¹ | Alhussain Yousef¹ | Panagiotis Spyridis^{1,2} | Frank Walther¹

Correspondence

Dr.-Ing. Ronja Scholz
TU Dortmund University
Chair Materials Test Engineering
Baroper Str. 303
D-44227 Dortmund
ronja.scholz@tu-dortmund.de
www.wpt-info.de

¹ TU Dortmund University,
Dortmund, Germany

² Rostock University, Rostock,
Germany

Abstract

In recent years, attention has been driven to the direct fastening technology by use of power actuated nail-type fasteners (PAFs) set in concrete. By means of the series of tests shown in this paper and the high-speed measuring equipment used, a first approach to the possibility of evaluating the setting performance is demonstrated. The difficulty is to judge whether the operation was successful and whether the fastening can bear the required force, since it is not possible to look into the concrete. For example, it remains hidden whether and, if so, how much the nail was deflected and bent by the concrete. Furthermore, it is unknown how the surrounding concrete was affected by occurring strains and heating as a result of friction. Since the setting process is very fast, it is necessary to use high-speed measurement technology. In the case of the studies conducted, both digital image correlation (DIC) and thermography were used to record material responses. Following the setting process, the nails and the surrounding concrete were separated and examined with computer tomography (CT). The CT provides the information on the inside of the concrete and one can see cracks and other reactions to the setting process.

Keywords

Direct fastening (nail-type), power actuated fasteners (PAF), fastening systems, high speed testing, setting process, digital image correlation, thermography.

1 Introduction and overview

A well-established fastening method is direct fastening by use of powder actuated fasteners (PAF), which bring along several benefits in terms of speed and ease of site work. However, due to the significant variability in the installation and load-bearing performance of such fasteners, particular focus needs to be diverted to the reliability characteristics and a redundancy-based design approach. The objective of the study is to provide fundamental engineering concepts for direct fastenings and to share and discuss the first worldwide experimental results on the validation of the setting performance of nail-type fasteners with high-speed measurement technology, in particular high-speed image correlation and thermography, complemented by computed tomography.

This paper provides some fundamental knowledge on the specific fastening technology and on the experimental tools and methods, it presents the measurement results and it concludes with first insights on the overall setting performance validation, conclusions for further research and technological developments as well as future prospects in the field.

2 Background knowledge on direct fastenings

Direct fastening is an efficient method, which provides facilitated fixing of steel bolts in concrete, steel, or wood. The load-bearing capacity of the directly fastened nail tends to show high scatter in the concrete as a result of the highly dynamic installation method and the randomness in localized consistency properties of concrete as a composite of cement in different crystallization phases and aggregates of different hardness, shape, size and orientation, as well as possible micro- or macro-cracking. Other influences include the inclusion and layout of reinforcement; in the present case steel fibers are used, but this can also refer to other types of fibers as well as bar and textile reinforcement of steel and other fiber reinforced polymer materials (e.g. carbon, basalt or glass fiber based).

The method of directly fastening to concrete using high-strength steel nails/bolts involves accelerating the fastener to speeds of up to 100 m/s using powder cartridges, compressed gas, or electrical spring mechanisms [1,2]. This technique offers advantages over conventional post-installed fastening systems in terms of time, cost, ergonomics, environmental conditions, and power supply.

However, direct fastening can result in significant scattering in terms of installation quality and load-bearing capacity due to immediate defects during the setting process, such as nail bents or breakage, as well as superficial concrete spalling and cracking [3,4]. Therefore, redundant fixing locations are often used to ensure load redistribution among participating fasteners [5-7]. A graph depicting the statistical distribution of pull-out loads of powder actuated fasteners in concrete is shown in Figure 1 (retrieved from [4] and modified), indicating a significant likelihood of setting failure of nearly 7%. The "stick rate," or the likelihood of achieving a firmness and a reliable pull-out resistance at setting, depends on the fastener product and the substrate and it typically ranges from 90-98% for standard concrete.

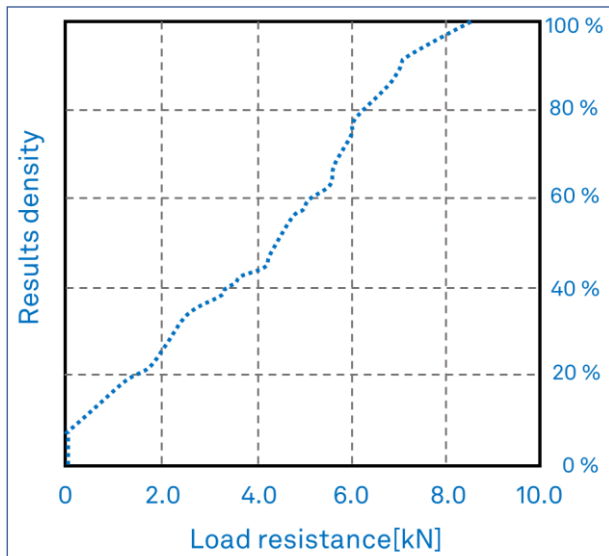


Figure 1 Indicative frequency density of pull-out loads of power actuated fastenings in unreinforced normal strength, standard aggregate concrete from test campaign in [4].

This technique fastening is commonly used for systems, such as pipes and electrical conduits, suspended ceilings, partition walls, architectural finishes, and auxiliary temporary works elements, which may be non-structural in nature but in many cases, they are safety-critical [2,8]. Therefore, understanding the existence of defects at installation is essential. Besides, application of this technique has also been proposed in research for load-bearing structures, particularly for attaching strengthening materials such as steel plates [9-10], shape memory alloys [11], and fiber-reinforced polymers [12], to enhance the resilience of damaged concrete structures. Furthermore, [13] indicates a good setting performance of such fasteners for textile-reinforced small-grain concrete elements with average and high compressive strength.

The anchoring mechanism of direct fasteners involves a frictional and clamping connection achieved through compaction and elastic confinement by the substrate through local radial compressive stresses, as well as interlocking through material sintering at the concrete-steel interface [1,3]. The setting mechanics have also been investigated on the basis of dynamic finite element calculations in [14,15], confirming the highly non-linear and random response of the fastener setting to various substrate conditions. These also showed the development of stresses,

compaction and plastification at the fastener's region. A theoretical performance of the material surrounding the nail is shown in Figure 2. Real marketed products, in particular those applied in the studies herein, are shown in Figure 3.

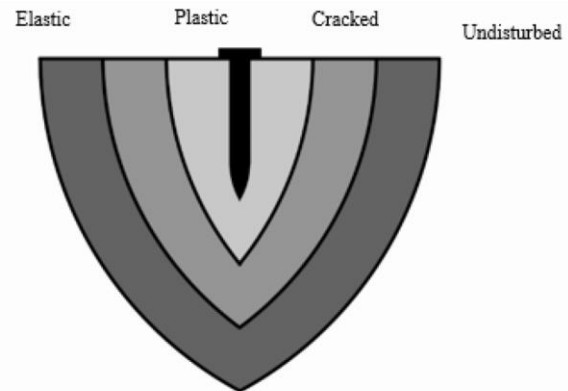


Figure 2 Theoretical model of the response regions in concrete at nail-type PAF installation (see also [14]).



Figure 3 Nail-type fasteners used in this study: round shank nail (left), and spiral shank nail (right)

3 Experimental approach

3.1 High-speed measuring technologies

Due to the fact that the setting process only takes a split second, it is difficult to record the material reaction resulting of the nail being shot into the concrete. To really see some reactions there is a need of measuring instruments, which can record at a sampling rate higher than a thousand pictures per second.

The first measuring technology used, was a high-speed camera with subsequent DIC analysis to record the strain, which is brought into the concrete. The system used was the Aramis HHS 3D of GOM, which has already been successfully used in previous investigations on composites [16,17]. It is able to record with a maximum frequency of $900,000 \text{ s}^{-1}$. The system consists of two identical cameras, which allow to capture a larger section of the concrete. The cameras have an internal memory with a capacity of 64 gigabyte. This results in a total amount of nearly 44,000 pictures that can be recorded and saved. Before doing the next recording, it is necessary to save the images on a local device. The setup of the two high-speed-DIC cameras and the additional lights is shown in Figure 4. The investigations of the nail setting process were carried out at a recording frequency of $22,500 \text{ s}^{-1}$.

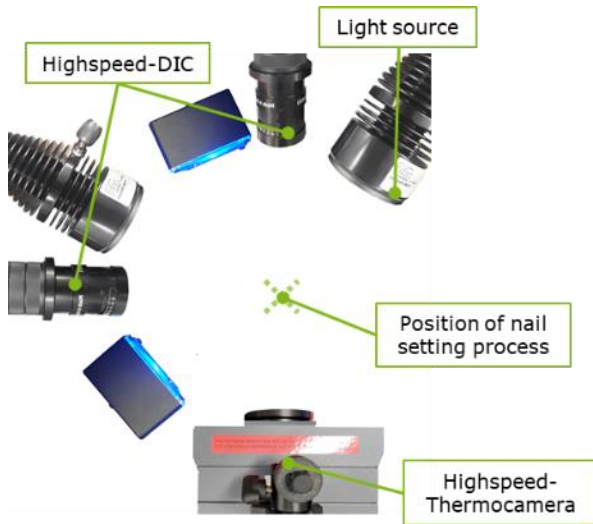


Figure 4 Experimental configuration for high-speed measurements.

The second measuring technology shown in Figure 4 is the high-speed thermography. The camera used is the ImageIR 8800 from InfraTec, which is able to record with a maximum frequency of $14,593 \text{ s}^{-1}$ at minimal frame size. When recording at the full screen size of 640×512 pixels there is a significant lower recording frequency of 233 s^{-1} . For the investigation purposes of the nail setting process the full screen recording is not fast enough. Therefore, the frame was minimized to a quarter frame (160×128 pixels), so that there was a maximum recording frequency of $2,500 \text{ s}^{-1}$ during the tests. The thermography camera is capable of recording in a temperature range of -40 to $1,200 \text{ }^\circ\text{C}$.

3.2 Pull Out tests

For the experimental investigations concrete specimens were cast with a composition of steel fiber reinforcement where used. In particular, the steel fibers used were of the commercial product Dramix by NV Bekaert SA, 4D 65/60BG [15]. The fibers are wire filaments of cold drawn wire with a diameter of 0.9 mm and hook-shaped ends, while their nominal material strength is 1600 MPa . As a consequence, the 4D steel fibers' efficiency is understood to be higher than 3D in crack bridging in terms of pull-out from the matrix as well as steel fiber rupture. The concrete mix was otherwise produced per testing standards for fastenings [18]. It is noted that, although measurements on single nails with CT and high-speed apparatus was conducted, at the time of this investigation and inception of this report, pull-out test series in plain concrete were unavailable. The concrete class was C20/25 with and 40 kg/m^3 steel fibers, Rhine River gravel including aggregates of $0/2 \text{ mm}$ at 36% , $2/8 \text{ mm}$ at 34% , and $8/16 \text{ mm}$ at 30% and with 235 kg/m^3 cement at a w/c ratio of 0.75 . On the form-work side each slab, 80 fasteners of each fastener type shown in Figure 3 were installed. Both these nail-type fasteners have a shank length of 27 mm and a diameter of 4 mm . For the pull-out tests, the fasteners were installed through a cored thin steel sheet adapter, which is laser cut and folded appropriately for the connection to the pull-out apparatus, as seen in Figure 5.



Figure 5 Installation set-up, using nail with light steel pull-out adapter and power actuated tool (top); Test configuration of pull-out test in two phases (bottom), indicating spalling at installation and bend nail at pull-out.

3.3 Computed tomography (CT)

After the setting process was done successfully, the concrete specimens were investigated using the technology of computed tomography. The scans were carried out on the XT H 160 of Nikon (Figure 6) that contains a microfocus X-ray tube with a maximum voltage of 160 kV . The specimen is located on a 5-axis manipulator that allows a full rotation of 360 degrees. The X-rays radiate the concrete specimen and are collected on a detector with a size of 1024×1024 pixels. Due to the rotation of the specimen multiple recordings of the specimen from a differing angle are taken, out of which a 3-dimensional volume can be reconstructed.

Because the concrete blocks in which the nails have been set were too massive to be radiated by the CT, it was necessary to drill out the nail and the surrounding concrete. Therefore, a core drill bit with a diameter of 60 mm was used to get the specimens in a fitting size as shown in Figure 6.

The aim of scanning the separated specimens was to detect cracks that were brought into the concrete due to the setting process of the nail. Furthermore, the starting point and the way the crack develops through the concrete should be imaged. In addition to that it is common, that the nail is deflected because of hitting rocks inside the concrete. With the help of the CT the angle of deflection could be investigated, which also has a direct impact on the success of the nail setting process and the ability of bearing the loadings occurring in application.



Figure 6 Computer tomography system and specimen.

4 Results and discussion

4.1 High-speed image-based measurements

The results of the measurement of the nail setting process are shown in the following. In the setting processes two different types of nails were compared to each other. With the contour of the spiral shaped nail it is anticipated to have a better penetration performance in concrete, but it is also expected that there will be more heat generation due to additional friction. Additionally, the concrete type was varied as previously mentioned.

Figure 7 shows the strain recorded via high-speed cameras with subsequent DIC-analysis exemplary for the combination of standard concrete and the round shank nail nail. First it can be seen that there was a slight difference in the calculated equivalent Mises strain ϵ_M in x- (section 2) and y-directions (section 1). The mean value of the strain for both directions is shown in Figure 7 as well. At the beginning of the testing procedure, the strain is around 0%, since the nail was not set into the concrete. With the nail being set, the strain for both sections increases abruptly. It can be seen, that the strain is around 1,5 % for both sections. The scattering is bigger for the x-direction, which can be attributed to the spalling of the concrete parts flying through the camera image, leading to calculation inaccuracies.

During the setting process of one of the nails the concrete showed a particularly stronger reaction in form of cracks going through the whole block of concrete. The resulting strains show a very remarkable progression as shown in Figure 8.

It is noticeable that the measured strains show an opposite reaction in both sections marked in Figure 8. A crack developed in the middle of the two areas as a result of the setting process. At the beginning of the recording the strain was 0% because the nail was not set. Immediately after the nail was set into the concrete the areas show a strongly differing reaction. While the lower area pulls apart, the concrete in the upper area contracts (Figure 8 (a)). As a result of the different directions of the strains, a crack emerges in between the two marked areas. With the opening of the crack, the strains in the areas turn into opposite directions (Figure 8 (b)). Now the lower area is contracted and the upper area pulls apart. The crack that appeared in the concrete block can be seen well in Figure 8 (b). The differing development of the strains for the previously mentioned areas is shown in Figure 8 as well.

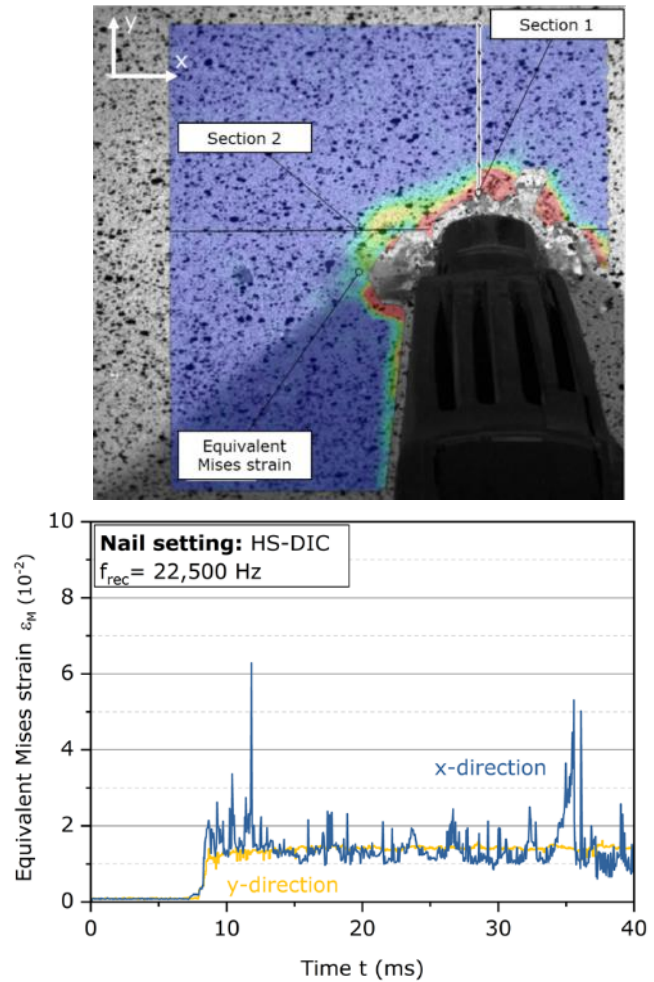


Figure 7 Exemplary representation of the strain measurement via high-speed-DIC, top: marked points for section 1 and 2 and bottom: calculated von Mises strain for the two sections.

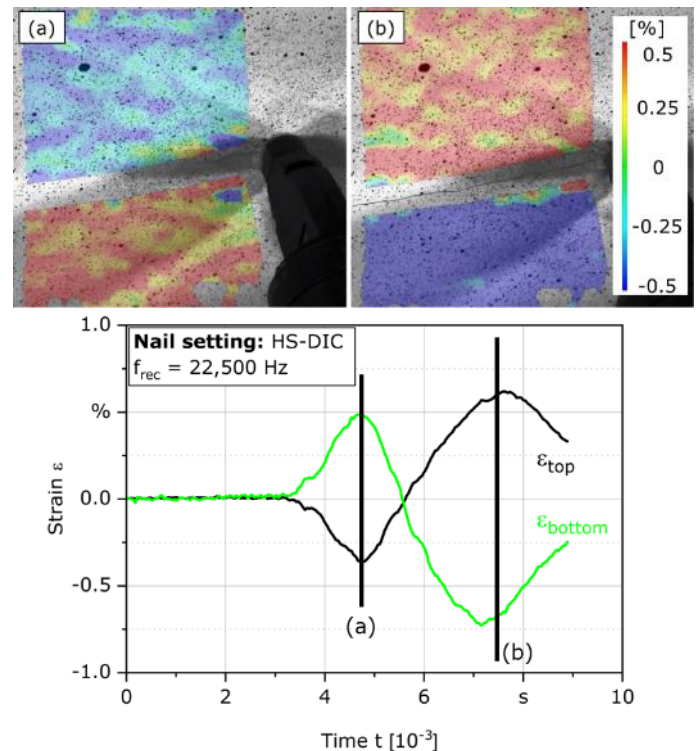


Figure 8 Measured strains of the nail setting process via high-speed camera with subsequent DIC analysis ((a) and (b)), and quantitative interpretation of results (bottom graph).

The results of the thermographic recordings of the setting process for the previously mentioned combinations of nail and concrete type are described in the following section. In Figure 9 (a) the maximum temperatures of the surrounding concrete immediately after the setting process are shown for the 4 different material combinations. It can be seen, that the maximum temperature was higher for the spiral shank nail. The highest temperature of around 130°C was recorded for the combination of the spiral shank nail and the fiber concrete. The high standard deviation shows that the maximum temperature was varying for this material combination. For the round shank nail the recorded maximum temperature was around 100°C for both of the types of concrete. The standard deviation was lower than the one for the previously mentioned material combination, making the temperatures for the round shank nails more comparable.

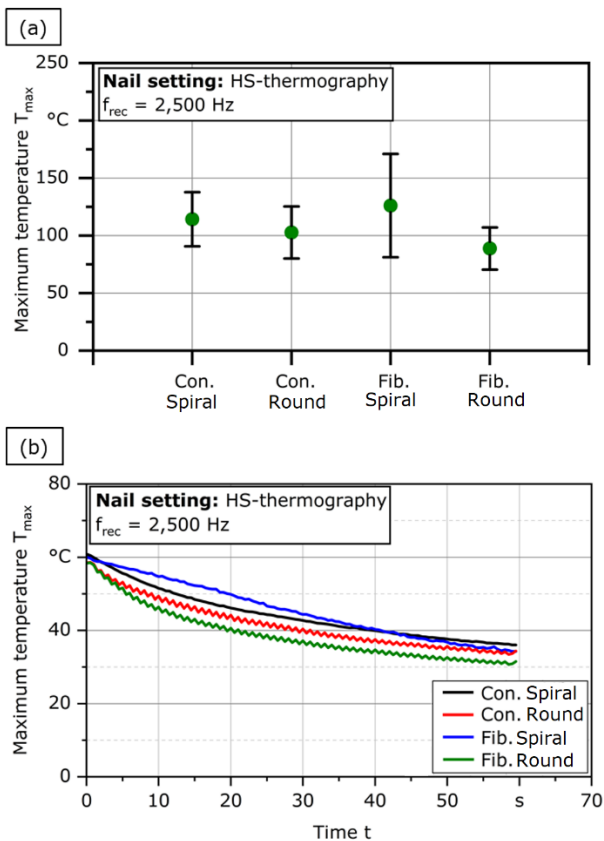


Figure 9 Temperature evolution following the nail setting process recorded via high-speed thermography, (a) maximum temperature and (b) cooling process in the first 60 seconds.

Figure 9 (b) shows the cooling process of the concrete surface surrounding the nail, recorded with a frequency of 2 Hz for the first 60 seconds. The cooling process again shows a difference between the two nails. In the first place, all material combinations start around a temperature of 60°C. After that, the round shank nail shows a stronger nearly exponential cooling in the first 30 seconds. The cooling of the surface surrounding the spiral shank nail is nearly linear compared to the round nail, leading to a higher surface temperature in the first 30 seconds for the spiral shank nail.

4.2 Statistical insights on setting/ pull-out tests

In parallel to the setting process investigations nails in

steel fiber reinforced concrete where tested in pull-out tests. The evaluation of the results was divided into two steps: the pre-testing evaluation and the post-testing evaluation. In the pre-testing evaluation, the obvious surface damage in the nail region spalling around the adapter was documented and classified in four categories. After this, the adapters were mounted to a hydraulic pull-out cylinder and tested in displacement-controlled mode at a constant speed of 0.02 mm/sec. Subsequently, the failure loads are statistically elaborated in the post-testing evaluation.

The assumed damage in the setting point vicinity is visually assessed and classified as follows:

- Class 0: no obvious damage
- Class 1: radial cracking with a finite length
- Class 2: circular cracking and surface spalling
- Class 3: setting failure, immediate loss of nail

As seen in Figure 10, stick rates were 100% and 97.5% for the round and spiral fasteners respectively. At the same time, the spiral fastener apparently has a better overall setting performance in terms of surface cracking/spalling, with 65% completely intact installations. These statistics hardly allow further distinction with respect to the nail-type, but by comparison to previous experiences in plain concrete – as for example also indicated in Figure 1 – a tendency is discerned that the setting performance in steel fibre concrete is superior to the ones obtained in plain concrete.

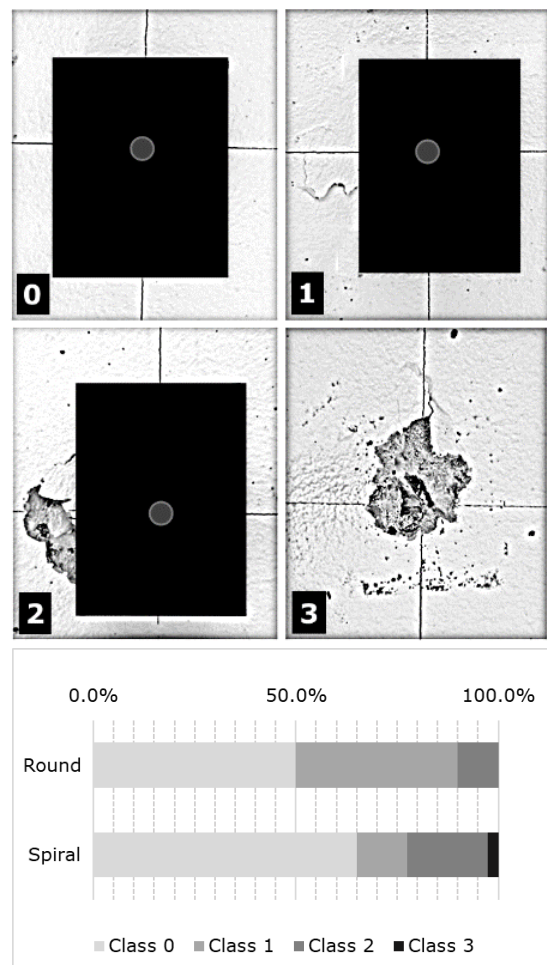


Figure 10 Top: sketched classification of nail setting performance beyond the nail and fixture (shaded area); bottom: frequency measurements in 80 nail setting series.

The data collected through pull-out testing refer to the maximum load. The loads are represented in Figure 11 in the form of cumulative density graphs. An overview of the results is also provided for clarity in Table 1: minimum value (excludes null due to setting failures), maximum and average values, the coefficient of variation and the statistical moments of standard deviation, skewness and kurtosis (the latter two are noted to merely complement the chosen best-fit distribution curves). A principal finding is that in none of the series the minimum load does approach null, which suggests that nails with apparent defects are likely to still entail a considerable load-bearing capacity in steel fibre concrete. The spiral nail fastener types yield generally higher values at average and maximum values compared to the round nail, but also somewhat higher scatter. The coefficients of variation are 22.4 and 32.3 for round and spiral nails respectively. It should be noted, that a full comparison of the variation and low load behaviour is difficult due to the limited sample size and low distribution density for lower quantiles.

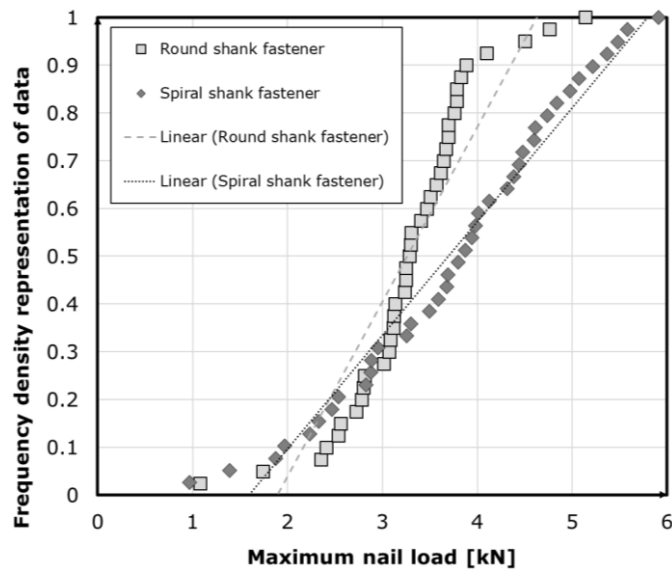


Figure 11 Cumulative frequencess of pull out load test results and indicative linear trendlines.

Table 1 Overview of statistical moments in pull-out load test results

Shank type	Min. [kN]	Max. [kN]	Ave. [kN]	St. D. [kN]	Kurt. [-]	Skew. [-]
Round	1.10	5.14	3.29	0.738	1.540	-0.312
Spiral	1.00	6.00	3.75	1.33	0.040	-0.601

4.3 Computer tomography investigations

Some of the nails were complementarily investigated in their post-setting condition using computer tomography. Figure 12 shows a comparison between the two types of concrete compared. On the left-hand side of the picture a spiral nail set into concrete without steel fibers can be seen. It is clearly visible that the nail has been deflected. However, it is not possible to determine the reason for the deflection by the recording shown in Figure 12. The figure also shows the top view of a nail set into the concrete with added steel fibers on the right. It becomes obvious that

the amount of fibers in the concrete is quite high and it can be assumed that the nail inevitable has to hit some of the fibers during the setting process.

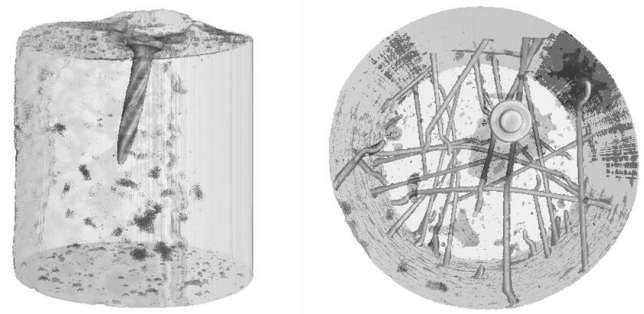


Figure 12 Comparison of the two types of concrete recorded via CT.

Figure 13 (a) shows two CT recordings for a standard concrete with the nail set into it. Once again, the deflection of the nail resulting from hitting a rock contained in the concrete. The angle of deflection can be measured at about 13-15°. Furthermore, there is a crack that can be seen in the CT recordings. It can be seen, that the crack initiation is located at bigger pores that are included in the concrete. The cracks run through the concrete towards further pores and at the edge of rocks inside the concrete.

Figure 13 (b) shows a recording of a nail set into the steel fiber concrete. In this particular case the nail hit a steel fiber and thereby it was deformed. Additionally, the nail was once more deflected by the impingement. Compared to the angle of deflection observed in Figure 13 (a) the deflection was not that significant in this case. The angle can be measured around 8-10°. Furthermore, the nail hit a big rock within the concrete. As a result of the impact energy, the rock was split apart which can be seen in the small cracks inside the substrate. The concrete shows no further cracks running through the whole specimen as observed in Figure 13 (a).

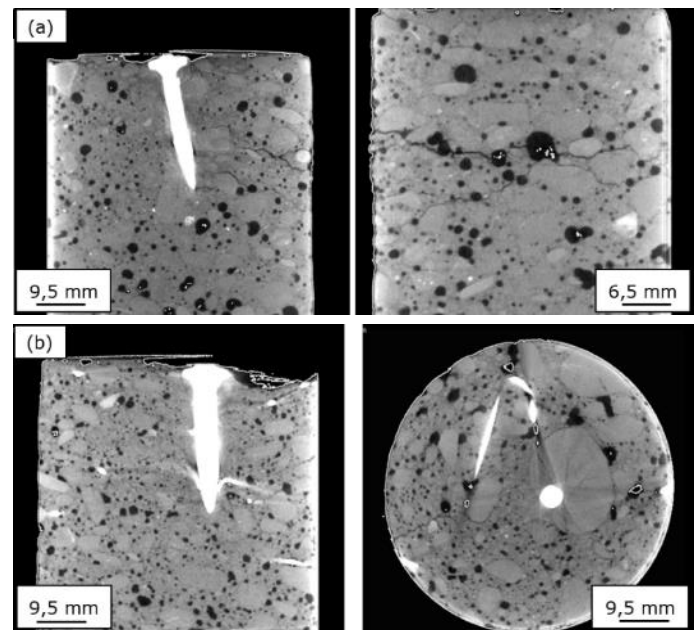


Figure 13 CT-scans of the effect of the nail setting process in (a) plain and (b) steel fiber reinforced concrete.

As seen, the fibers intersect the nail. It was not possible to identify if the fibers are simply sheared and separated by the nail or if there is also some mechanical connection and load transfer between the two elements, e.g. through cindering and fusion or high friction. In any case, however, the inclusion of steel fibers is expected to have an effect to the setting and pull-out procedure and mechanisms.

5 Conclusions

Direct fastening using nail-type powder actuated fasteners (PAF) is a well-established method that offers advantages in terms of speed and convenience in a range of construction and building applications. Due to the specific installation method, fasteners tend to exhibit a significant variation in their pull-out resistance, whilst it is also typical to have a small portion of the fastenings failing immediately at installation. This leads to a requirement for special attention to reliability and the use of redundancy-based design strategies.

To enhance the understanding of these installation mechanisms and their potential association with low load capacities, a series of tests has been carried out and enhanced observation and measuring methods are employed and demonstrated herein. The study leads to the following conclusions on the setting and pull-out behaviour as well as the various implemented laboratory techniques:

- The nail type and the concrete substrate mix (particularly unreinforced or fibre reinforced) are shown to have an influence on the setting and load-bearing performance of the fasteners. It is anticipated that fibre reinforcement reduces the likelihood of failure at installation significantly in relation to previous tests in unreinforced concrete from the literature.
- High-speed-DIC analysis: The possibility of recording strains brought into the concrete as a result of the nail setting process could be confirmed, though spalling of the concrete leads to calculation inaccuracies.
- High-speed-thermography: The measurement technology gives information about the temperature brought into the concrete after setting the nail. Since the setting device blocks the view on the point of interest, the first split seconds of the temperature development could not be recorded.
- Computer tomography (CT): By means of radiating the specimen, valuable information on the success of the nail setting process could be gathered. The status of the concrete as well as the angle of deflection could be visualized using CT.
- Spiral shank fasteners tend to have a better setting overall performance compared to round shank fasteners. This is also reflected in the higher pull-out loads on average.

In order to improve understanding of this fastening system and provide reliable practical recommendations, additional research must be conducted. From a statistical viewpoint,

it may be necessary to expand the sample size of the tested dataset to 60–80 probes or more per test parameter, so as to enhance the precision of statistical assessments. Further trials of high-speed testing methods may deliver useful results but some adjustments need to be made in the testing equipment. The scope of this study could not entail a great number of tests at this stage, but it will be useful to collect further data and their association with pull-out loads. Besides, further structural and material mix parameters of the concrete should be accounted for, since they are decisive for the overall performance. This approach may lead to both enhance knowledge in the testing phase but also to the possibility of performance assessment directly on the site.

Acknowledgments

The authors thank the German Research Foundation (DFG, Deutsche Forschungsgemeinschaft) and the Ministry of Culture and Science of Northrhine-Westphalia (Ministerium fuer Kultur und Wissenschaft des Landes Nordrhein-Westfalen, NRW) for their financial support within the Major Research Instrumentation Programs for the high-speed camera system (project-no. 424852613, INST 212/428-1 FUGG) and for the high-speed thermography system (project-no. 444290516, INST 212/459-1 FUGG).

The authors further thank the following organizations for their in-kind and technical contributions: The steel fibres used were kindly provided by NV Bekaert SA. The fastening tools and expendables were offered by Hilti Corporation. The laser cutting of the metal sheet adapters was delivered by the Institute of Forming Technology and Lightweight Components of the TU Dortmund University.

References

- [1] Eligehausen, R., Mallée, R., Silva, J. F. (2006). *Anchorage in concrete construction*. Berlin: Ernst & Sohn.
- [2] Hilti Corporation (2019). *Direct fastening technology manual 2019. Online manual of fastening technology*. Schaan: Hilti Deutschland.
- [3] Bergmeister, K. (1988). *Stochastik in der Befestigungstechnik mit realistischen Einflussgrößen*. Dissertation, University of Innsbruck, Faculty of Civil Engineering and Architecture, Innsbruck.
- [4] Gerber, W. (1987). *Theorie zum Eintreiben und Verankern von Bolzen in Beton*. Bauingenieur 62, 213–218.
- [5] Patzak, M. (1979). *Zur Frage der Sicherheit von Setzbolzenbefestigungen in Betonbauteilen*. Beton + Fertigteil-Technik 5/1979, Wiesbaden: Bauverlag.
- [6] EAD 330083-02-0601. (2018). *Power-actuated fastener for multiple use in concrete for non-structural applications*. Brussels: EOTA.
- [7] DIN CEN/TR 17079 (2019). *Design of anchorage of fastening systems in concrete - Redundant non-load-bearing systems*. Berlin: Beuth Verlag.

- [8] Gould, W., Lichti, D. (2013) *Power Forward: Diving power-actuated fastener (PAF) code provisions*. STRUCTURE magazine, Illinois: Structure.
- [9] Shan, Z. W., Looi, D. T. W., Su, R. K. L. (2020). *A novel seismic strengthening method of RC columns confined by direct fastening steel plates*. Engineering Structures, 218, 110838.
- [10] Su, R. K. L., Shan, Z. W. (2019). *Axial strengthening of RC columns by steel encasement with direct fastening connection*. IOP Conference, Material Science and Engineering.
- [11] Michels, J., Shahverdi, M., Czaderski, C. (2018). *Flexural strengthening of structural concrete with iron-based shape memory alloy strips*. Structural Concrete 19(3), fib, Berlin: Ernst & Sohn.
- [12] Lamanna AJ, Bank LC, Scott DW. (2004). *Flexural strengthening of reinforced concrete beams by mechanically attaching fiber-reinforced polymer strips*. Journal of composites for construction, 8(3):203-10.
- [13] Langenbeck, A. D., Spyridis, P., Beßling, M., & Orłowski, J. (2023). *Experimental investigations of power-actuated fastenings in TRC*. Developments in the Built Environment, 100158.
- [14] Mellios, N., Bushra, M., Yousef, A., Spyridis, P. (2022). *Probabilistic finite element investigation of direct fasteners in concrete with discrete aggregates*. Proceedings of the 14th fib PhD Symposium (eds. Di Prisco, M., Meda, A., Balázs, G.L.), Rome, Italy, 5-7 September 2022.
- [15] Yousef, A., Mellios, N., Spyridis, P. (2022). *Probabilistic finite elements of direct fixings in concrete with discrete steel-fibers*. Proceedings of the 14th fib PhD Symposium (eds. Di Prisco, M., Meda, A., Balázs, G.L.), Rome, Italy, 5-7 September 2022.
- [16] Gerdes, L., Richle, S., Mrzljak, S., Hülsbusch, D., Barandun, G., Walther, F. (2022). *Computed tomography-based characterization of impact and fatigue after impact behavior of carbon fiber-reinforced polyurethane*. Composite Structures 289, 115474.
- [17] Gerdes, L., Franck, P., Richle, S., Barandun, G. A., Walther, F. (2023). *Fatigue assessment of carbon fiber-reinforced polyurethane with regard to crack initiation and propagation*. Eng, 4(2), 1009-1022.
- [18] NV Bekaert SA (2019). *EC Declaration of performance DRAMIX® 4D 65/60BG*. <http://www.bekaert.com/en/product-catalog> (accessed 18-12-2022).
- [19] EOTA – European Organisation for Technical Approvals (2016). Technical report TR 048 “*Details of tests for post-installed fasteners in concrete*”. Brussels.